Available online at www.sciencedirect.com
ScienceDirect
Biochimica et Biophysica Acta 1768 (2007) 299–310
Biochimica et Biophysica Acta BBA
www.elsevier.com/locate/bbamem

Visualizing the localization of sulfoglycolipids in lipid raft domains in model membranes and sperm membrane extracts

Wattana Weerachatyanukul [a,1], Ira Probodh [a], Kessiri Kongmanas [b], Nongnuj Tanphaichitr [b,*], Linda J. Johnston [a,*]

[a] *Steacie Institute for Molecular Sciences, National Research Council Canada,100 Sussex Drive, Ottawa, ON Canada K1A 0R6*
[b] *Hormones/Growth/Development, Ottawa Health Research Institute, and Departments of Obstetrics/Gynecology and Biochemistry/Microbiology/Immunology, University of Ottawa,725 Parkdale Ave, Ottawa, ON Canada K1Y 4E9*

Received 9 June 2006; received in revised form 17 August 2006; accepted 28 August 2006
Available online 15 September 2006

Abstract

Sulfogalactosylglycerolipid (SGG) is found in detergent-resistant lipid raft fractions isolated from sperm plasma membranes and has been shown to be important in sperm–egg adhesion. In order to provide more direct evidence for the association of sulfoglycolipids with lipid raft domains, we have examined the distribution of two sulfoglycolipids in supported membranes prepared from artificial lipid mixtures and cellular lipid extracts. Atomic force microscopy has been used to visualize the localization of SGG and sulfogalactosylceramide (SGC) in liquid-ordered domains in supported bilayers of ternary lipid mixtures comprised of dipalmitoylphosphatidylcholine, cholesterol and palmitoyldocosahexaenoylphosphatidylcholine. The localization of SGC/SGG in the liquid-ordered raft domains is demonstrated by changes in bilayer morphology in the presence of sulfoglycolipid, by selective antibody labeling of the domains with anti-SGC/SGG and by the effects of the cholesterol-sequestering agent, methyl-β-cyclodextrin, on the supported membranes. In addition, we use a combination of atomic force microscopy and immunofluorescence to show that supported bilayers made from lipids extracted from sperm anterior head plasma membranes (APM) and isolated APM vesicles exhibit small SGG-rich domains that are similar to those observed in bilayers of artificial lipid mixtures. The possible implications of these results for the involvement of SGG-rich lipid rafts in modulating sperm–egg interactions *in vivo* and the utility of model membranes for studying the behavior of lipid rafts are discussed.

Keywords: Lipid rafts; Membrane; Atomic force microscopy; Fluorescence; Sulfoglycolipid

1. Introduction

Plasma membrane microdomains known as lipid rafts have been proposed to facilitate the assembly of signaling and cell adhesion complexes and to regulate membrane trafficking [1–3]. Rafts are enriched in saturated lipids, cholesterol and certain glycolipids and proteins and are generally believed to exist in a liquid-ordered phase characterized by tight packing of lipid acyl chains and lateral diffusion properties similar to those of a fluid phase. Much of the original evidence in support of raft domains came from the isolation of a specific set of lipids and proteins from plasma membranes using cold nonionic detergents [4]. However, it is not straightforward to correlate these detergent-resistant membrane fractions with pre-existing domains in cellular membranes. The direct detection of rafts in cells has proven a challenge, in large part due to their small size and dynamic nature. This has resulted in a number of different models to explain membrane compartmentalization and a general lack of consensus on the size, formation and

Abbreviations: AFM, atomic force microscopy; APM, anterior head plasma membrane; chol, cholesterol; DPPC, dipalmitoylphosphatidylcholine; HPTLC, high performance thin layer chromatography; l_o, liquid-ordered; MβCD, methyl-β-cyclodextrin; NCM, non-capacitation medium; PC, phosphatidylcholine; PDPC, palmitoyldocosahexaenoylphosphatidylcholine; PRS, preimmune rabbit serum; SGC, sulfogalactosylceramide; SGG, sulfogalactosylglycerolipid; SM, sphingomyelin; TLC, thin layer chromatography

* Corresponding authors.
E-mail addresses: ntanphaichitr@ohri.ca (N. Tanphaichitr), Linda.Johnston@nrc-cnrc.gc.ca (L.J. Johnston).
[1] Permanent address: Department of Anatomy, Faculty of Science, Mahidol University, Rama VI Road, Bangkok 10400, Thailand.

0005-2736/$ - see front matter. Crown Copyright © 2006 Published by Elsevier B.V. All rights reserved.
doi:10.1016/j.bbamem.2006.08.022

function of lipid rafts [5–11]. It is clear that new experimental approaches capable of probing membrane compartmentalization on a variety of length and time scales are required to rationalize these diverging views.

The challenge of detecting lipid rafts in cellular membranes has motivated many studies of artificial lipid mixtures that mimic some of the properties of rafts and detergent-resistant membranes. Model membranes such as phospholipid vesicles and supported monolayers and bilayers have been examined using a variety of spectroscopic and microscopic methods and have provided valuable information on the phase behavior of lipid mixtures [11,12]. For example, methods such as fluorescence microscopy frequently provide evidence for relatively large liquid-ordered raft domains rather than the small nanodomains that are believed to be important in natural membranes, whereas studies using fluorescence energy transfer provide evidence for much smaller nanodomains. We have previously used atomic force microscopy (AFM) to study domain formation in monolayers and bilayers of binary and ternary lipid mixtures and to examine the distribution of the *in vivo* raft marker GM1 in various supported membranes [13–18]. AFM has the potential to resolve domains on a wide range of length scales, from tens of nanometers to tens of micrometers under close to "physiological" conditions and, when combined with immunofluorescence imaging, can be applied to studies of nanodomains in cellular membranes [19,20]. Supported lipid bilayers have been widely used as membrane models since they retain activity of reconstituted proteins, have significant lipid mobility and are amenable to characterization with a range of surface techniques [21]. The lateral lipid mobility is largely due to the thin water layer (1–2 nm) separating the bilayer from the solid support and effectively allows for decoupling of the membrane from the support.

In the present study we have examined the distribution of two sulfoglycolipids in liquid-ordered raft domains in supported membranes prepared from both artificial lipid mixtures and cellular lipid extracts. Both sulfogalactosylglycerolipid (SGG) and sulfogalactosylceramide (SGC) have primarily saturated acyl chains and have a propensity to interact with themselves and with cholesterol and saturated phospholipids [22–24]. SGC is found in male germ cells of lower vertebrates and invertebrates, and the myelin sheath and epithelial cells of the kidney and digestive tract in mammals [24] and has been shown to be a component of lipid rafts from MDCK cells [25] and sea urchin sperm [26]. The structural analog SGG is found in mammalian male germ cells [24,27]. Recently, we have demonstrated that the majority of SGG in capacitated pig sperm is isolated in detergent-resistant membranes which bind the egg extracellular glycoprotein matrix, the zona pellucida (ZP) [28]. SGG liposomes exhibit strong binding to zona pellucida [28–30], indicating that the sulfoglycolipid contributes significantly to the zona pellucida binding ability of isolated sperm lipid rafts. The mechanisms utilized by sperm lipid rafts to bind to the zona pellucida appear to be similar to those employed by intact sperm, suggesting that lipid rafts mediate the initial sperm egg interaction [28]. Since these studies were all based on the use of isolated detergent-resistant membranes, the present study was undertaken to provide more direct evidence for the presence of SGG in liquid-ordered raft domains.

Herein we use AFM to demonstrate that SGC and SGG localize in liquid-ordered raft domains in bilayers of artificial lipid mixtures that mimic the composition of sperm plasma membranes. We also use a combination of AFM and immunofluorescence microscopy to show that SGG localizes in similar domains in bilayers prepared from lipids extracted from the sperm anterior head plasma membrane (APM) and isolated APM vesicles. These observations provide a better understanding of the role of SGG in the formation of sperm lipid rafts, and consequently the potential involvement of these sperm lipids in sperm–egg interaction. They also highlight the utility of model systems for mimicking at least some of the properties attributed to lipid rafts in biological membranes.

2. Materials and methods

2.1. Lipids

Glycerophospholipids and cholesterol (chol) were purchased from Avanti Polar Lipids (Alabaster, AL). Pig brain SGC (consisting of 60% hydroxylated and 40% non-hydroxylated forms [31]) was ordered from Sigma (St. Louis, MO) and further purified by preparative thin layer chromatography (TLC), using chloroform/methanol/water (65:24:4, v/v/v) as the solvent system [32]. SGG was purified from pig testes following our described method [33]. Endogenous cations of both SGC and SGG were removed and replaced by Na^+ as described previously [33]. The purity of SGG and SGC was verified by high performance thin layer chromatography (HPTLC) using the same solvent system described above. SGG appeared as a single band with a relative R_f value of 0.329 and SGC as a doublet with relative R_f values of 0.3 (hydroxylated form) and 0.325 (non-hydroxylated form).

2.2. Preparation of lipids from pig sperm anterior head plasma membrane (APM)

Ejaculated semen samples collected from mature fertile boars were diluted in Beltsville Thawing Solution (BTS: 0.2 M glucose, 20 mM sodium citrate, 15 mM $NaHCO_3$, 3.36 mM Na_2EDTA, 10 mM KCl, 8 mM Na_2HPO_4, 2 mM NaH_2PO_4, and 1 mg/ml dihydrostreptomycin, pH 7.4) and stored (18 °C, <24 h) in dark until use. These diluted semen samples were provided by Dr. M Buhr, University of Guelph, ON, Canada. Sperm, washed free of seminal plasma by centrifugation (350 ×*g*, 28 °C, 10 min), were resuspended at 1×10^9 sperm/ml in non-capacitation medium (NCM: 0.1 M NaCl, 0.36 mM NaH_2PO_4, 8.6 mM KCl, 0.5 mM $MgCl_2$, 11 mM glucose, 23 mM HEPES, pH 7.6) [34]. Motile sperm populations were prepared by density gradient (35% and 70% Percoll diluted in NCM) centrifugation (600×*g*, 28 °C, 30 min) [35], and washed once in NCM before incubation (5% CO_2, 39 °C, 2 h) in CM (NCM plus 10 mM $NaHCO_3$, 2 mM $CaCl_2$, 5 mM pyruvate and 0.3% BSA [34]) at 10×10^6 sperm/ml. More than 90% of these gametes possessed hyperactivated motility patterns typical of capacitated sperm. They were then washed twice with NCM, resuspended at a concentration of 0.4×10^9 sperm/ml in pre-chilled Tris-buffered sucrose solution (TBSS: 5 mM Tris–HCl, pH 7.4, 0.25 M sucrose) and subjected to nitrogen cavitation (650 psi, 10 min), using a Parr cell disruptor (Pars Instrument Company, Moline, IL), immersed in an ice bath [36]. Following low speed centrifugation to pellet sperm particulates, APM vesicles in the supernatant were collected and then subjected to ultracentrifugation (117,730×*g*, 4 °C, 90 min) in a 70 Ti rotor (Beckman, Palo Alto, CA). The pelleted APM vesicles were washed once at the same ultracentrifugation speed with HEPES-buffered saline (HBS: 5 mM HEPES, pH 7.4, 2.7 mM KCl, 146 mM NaCl) to remove sucrose, and resuspended in 1 ml of HBS. Lipids were extracted from these APM vesicles by a modified Bligh-Dyer's method [37,38].

2.3. Preparation of affinity purified anti-SGC(SGG) IgG/Fab

Rabbit polyclonal anti-SGC/SGG IgG antiserum was produced and the IgG fraction was purified as described previously [29]. IgG was purified from preimmune rabbit serum (PRS). Affinity purified anti-SGC/SGG IgG was prepared based on its affinity for SGC multilamellar liposomes. SGC matrices were used for the purification, since the antibody also recognizes SGG due to the similarity of their structures [29]. Briefly, the IgG fraction purified from anti-SGG/SGC antiserum was incubated (2 h, room temperature) with SGC liposomes with a molar ratio of 1:100. The IgG-liposome complexes were ultracentrifuged (200,000×*g*, 1 h, 4 °C). The bound IgG, i.e., affinity purified anti-SGG/SGC IgG, was eluted from the liposomes by treatment with 0.6 M KI followed by ultracentrifugation (200,000×*g*, 1 h, 4 °C) to pellet the SGC liposomes. Affinity purified anti-SGG/SGC IgG in the supernatant was collected, dialyzed against 1 mM Tris–HCl, pH 7.4, lyophilized, and then reconstituted in PBS for use.

2.4. AFM of supported bilayers of artificial lipid mixtures and sperm APM lipids

Lipid mixtures of dipalmitoylphosphatidylcholine (DPPC)/palmitoyldocosahexaenoylphosphatidylcholine (PDPC)/chol (4:4:2, molar ratio) were dissolved in chloroform in the presence or absence of SGC or SGG. Sulfoglycolipid-containing samples were prepared with 4.7 or 9.1% SGC (giving final DPPC/PDPC/chol/SGC molar ratios of 4:4:2:0.5 and 4:4:2:1, respectively) and 9.1 mol% SGG (DPPC/PDPC/chol/SGG molar ratio of 4:4:2:1). The lipids were dried under a nitrogen stream and further dried under vacuum overnight. Milli-Q water was added to the dried lipids to give a final concentration of 1 mg/ml. The samples were vortexed and then sonicated for 10 min using a probe sonicator (output=9 W, pulse=3 s, pause=1 s) (Cole and Palmer, Vernon Hills, IL) to give a clear lipid vesicle suspension. Particles remaining in the suspension were pelleted by centrifugation (12,000×*g*, 10 min, room temperature). The lipid vesicle solution was mixed with an equal volume of 100 mM $CaCl_2$ in an AFM fluid cell. The vesicles were allowed to fuse (30 min, room temperature) onto a freshly cleaved mica sheet to form supported bilayers. The samples were washed extensively with Milli-Q water to remove unfused vesicles. AFM images of supported bilayers were acquired in aqueous solution using a Mac Mode PicoSPM atomic force microscope (Molecular Imaging, Phoenix, AZ) with magnetic coated cantilevers (MAC levers, Type II, Molecular Imaging) with silicon tips (spring constant=0.1 N/m). Images were recorded with the minimum force possible and the scan speed was <5000 nm/s. Images of 2 or 3 macroscopically different areas of each sample were recorded and a minimum of two independently prepared samples were imaged for each bilayer composition. Control experiments in which all steps in the vesicle fusion and bilayer formation were carried out in a nitrogen atmosphere indicated that the bilayer morphologies for the ternary lipid mixtures alone and in the presence of SGC/SGG are similar for samples prepared under air and nitrogen. This indicates that any oxidized lipid that may be formed in the bilayer samples prepared under air do not affect the overall results.

The preparation of sperm lipid vesicles and supported bilayers and their AFM imaging were carried out using the methods described above for the ternary lipid mixtures.

2.5. Localization of SGC/SGG in supported lipid bilayers

Supported bilayers of quaternary lipid mixtures (DPPC/PDPC/chol/SGC (SGG) at a molar ratio of 4:4:2:1) or APM lipid extracts were prepared and imaged in Milli-Q water as described above. The water in the AFM cell was then replaced with 50 mM HEPES buffer, pH 7.4 for 5 min prior to incubation (30 min, room temperature) with 0.2–0.5 μg/ml affinity purified anti-SGG IgG. After an extensive wash with Milli-Q water to eliminate unbound antibody, AFM images from different areas were acquired at the lowest force that allowed stable imaging. The following negative controls were also imaged: (1) DPPC/PDPC/chol/SGC(SGG) bilayers incubated with PRS IgG at the same concentration as anti-SGG IgG, and (2) DPPC/PDPC/chol bilayers (without SGC or SGG) incubated with anti-SGG IgG.

2.6. Methyl-β-cyclodextrin (MβCD) treatment of lipid bilayers

Supported bilayers of sperm APM extracts and mixtures of pure lipids were prepared as described above and imaged by AFM in Milli-Q water. The lipid bilayers were then incubated with 10 mM MβCD in Milli-Q water (15 min, room temperature) and washed with water prior to imaging. In some cases, bilayers were imaged without washing, leading to continued changes in bilayer morphology due to longer exposure times to MβCD.

2.7. Immunofluorescence of APM bilayers

Bilayers of APM vesicles and lipid extracts were constructed on a thin mica sheet placed over a 13-mm hole in a slide holder under the same conditions described above for wet AFM imaging. After washing, the bilayers were treated with 0.5 μg/ml affinity purified anti-SGG IgG in 50 mM HEPES, pH 7.4 (30 min, room temperature), washed, and subsequently exposed to 1 μg/ml Alexa-488 conjugated goat anti-rabbit IgG in the same buffer (30 min, room temperature). The bilayers were then washed with Milli-Q water and viewed using a Bio-Rad MRC-1024 Laser Scanning Confocal Microscope (Bio-Rad Laboratories, Hercules, CA) equipped with an argon ion laser and mounted on an Olympus IX70 inverted microscope (Olympus, Millville, NY). All images were captured with a 60× oil immersion (NA=1.4) objective using a fluorescein filter set (excitation and emission wavelengths of 488 and 520 nm, respectively) under a slow scanning mode. Controls were bilayers prepared as described above and exposed to PRS IgG under the same conditions as bilayers treated with anti-SGG IgG. The sizes of immunoreactive domains were measured using a section analysis mode and Image J1.27z software downloaded from http://rsb.info.nih.gov/ij/, and were reported as full width at half maximum intensity.

3. Results

3.1. Distribution of sulfoglycolipids in DPPC/PDPC/chol lipid bilayers

Both supported membranes [39–45] and vesicles [46–50] prepared from ternary lipid mixtures comprised of a saturated phosphatidylcholine (PC) or sphingomyelin (SM), an unsaturated PC and cholesterol have been widely used as models for the behavior of lipid rafts in natural membranes. These mixtures typically have two coexisting liquid phases, a liquid-ordered phase rich in cholesterol and saturated PC or SM and a liquid-disordered phase rich in the low melting unsaturated PC. In the present work we investigated the distribution of sulfoglycolipids SGC and SGG in PDPC/DPPC/chol (4:4:2) bilayers as a model system. The choice of DPPC and the DPPC/chol ratio is based on our recent results which found a SGG/chol/phospholipid molar ratio of 1:2:4 in isolated pig sperm lipid rafts, with PC being the major phospholipid and most acyl chains being C16:0 [28]. Since sperm contain substantial amounts of phospholipids with long-chain polyunsaturated fatty acids [51], PDPC was selected as the unsaturated PC component of the model system. The use of equal amounts of saturated and unsaturated PCs gives similar amounts of raft and fluid phases, as described below.

As shown in Fig. 1A, the DPPC/PDPC/chol mixture gives a phase-separated bilayer with large raised domains that are 1.6± 0.1 nm higher than the surrounding fluid phase. There are occasional small defects in the lower phase (arrows in Fig. 1A), clearly indicating the presence of a phase-separated bilayer, as opposed to membrane patches surrounded by bare mica. The

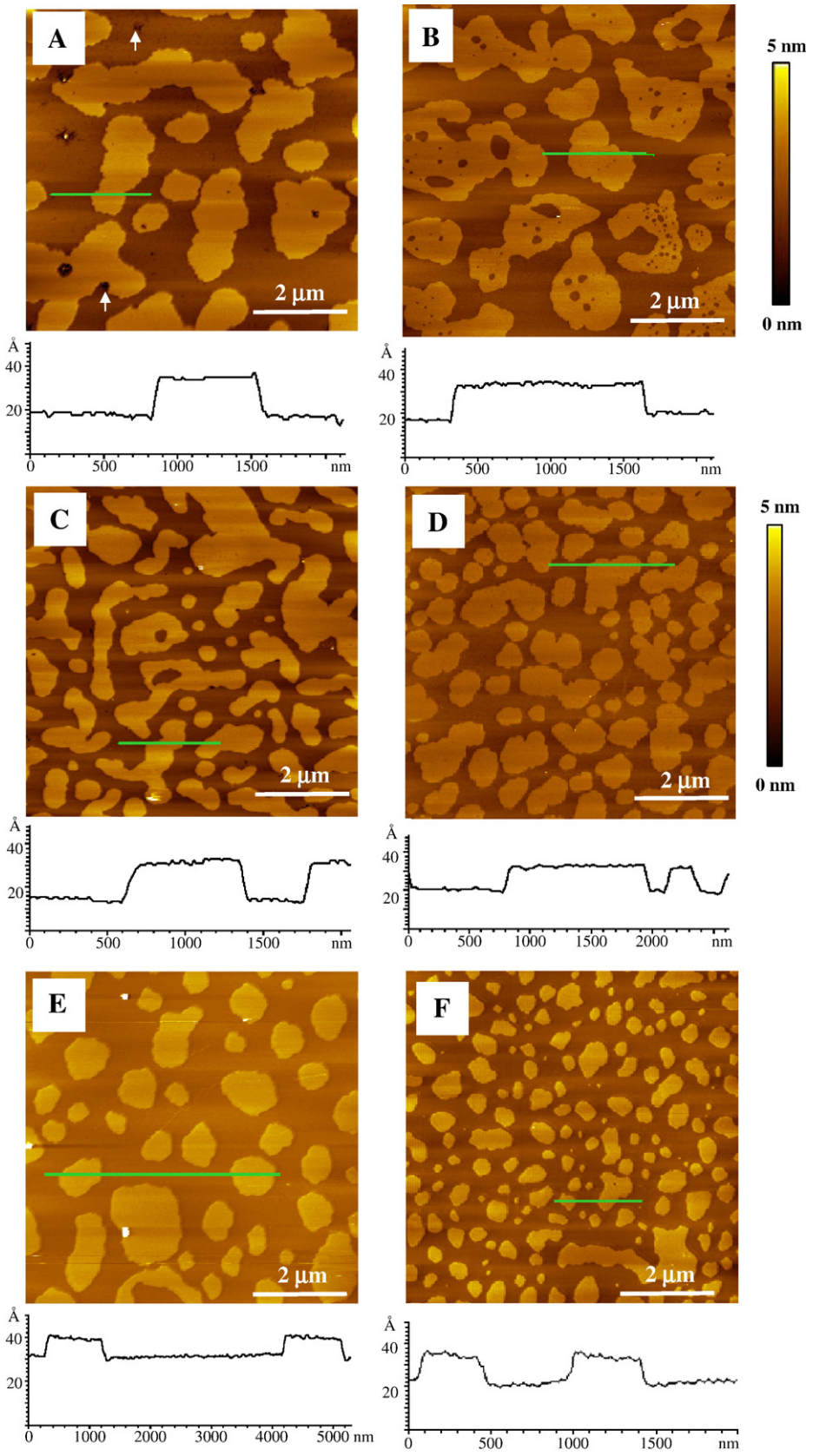

Fig. 1. Morphology of DPPC/PDPC/cholesterol bilayers in the presence and absence of SGC and SGG. Atomic force microscopy images in aqueous solution for supported bilayers with the following compositions (molar ratios): (A) 4:4:2 DPPC/PDPC/chol, (B) 4:4:2:0.5 DPPC/PDPC/chol/SGC (4.7% SGC), (C) 4:4:2:1 DPPC/PDPC/chol/SGC (9.1% SGC), (D) 4:4:2:1 DPPC/PDPC/chol/SGG, (E) 4:4:2 DPPC/DOPC/chol and (F) 4:4:2:1: DPPC/DOPC/chol/SGG. Cross-section analyses for the lines are shown beneath the individual images. The arrows in panel A indicate bilayer defects.

raised domains are somewhat irregular in both size and shape (0.4–3 μm); the shape of some larger domains suggests that they are formed by coalescence of two or more smaller domains. Both the degree of interconnectivity between domains and their size and shape vary somewhat from sample to sample and with the area imaged (a comparison of Fig. 1A to images in Figs. 2D and 4A shows the type of variation typically observed for this mixture). The domain boundaries are reasonably smooth as expected for liquid-ordered domains [52]. Based on similar results in other ternary lipid mixtures, we assign the higher domains to a liquid-ordered (l_o) DPPC/cholesterol-rich phase and the surrounding bilayer matrix to a fluid PDPC-rich phase [41,42,45,53].

Addition of SGC to the ternary lipid mixture leads to changes in the bilayer morphology as shown in Fig. 1B and C for bilayers with 4.7 and 9.1% SGC. Bilayers containing 4.7% SGC have domains that frequently contain small microdomains of fluid phase that are trapped when small domains coalesce during vesicle rupture and spreading. At the higher concentration of sulfoglycolipid the raised domains are considerably smaller (0.2–2 μm) with branched and interconnected structures. Relatively few trapped islands of fluid phase are observed, presumably since there are fewer large domains for this mixture. Although the average domain height (1.6±0.2 nm for multiple images and several independent bilayer preparations) is similar to that for the ternary lipid mixture, there is more variation in height within individual domains, indicative of a non-uniform distribution of lipids within the domain. Fig. 1D shows a typical image obtained upon addition of SGG to DPPC/PDPC/chol bilayers. The size of the raised domains is smaller (~0.2–1 μm) and the domains are less interconnected, compared to bilayers containing the same amount of SGC. The height difference between the domains and fluid phase decreases slightly (1.3±0.2 nm). The changes caused by addition of sulfoglycolipid are clearly larger than the variation observed for multiple samples of the same composition.

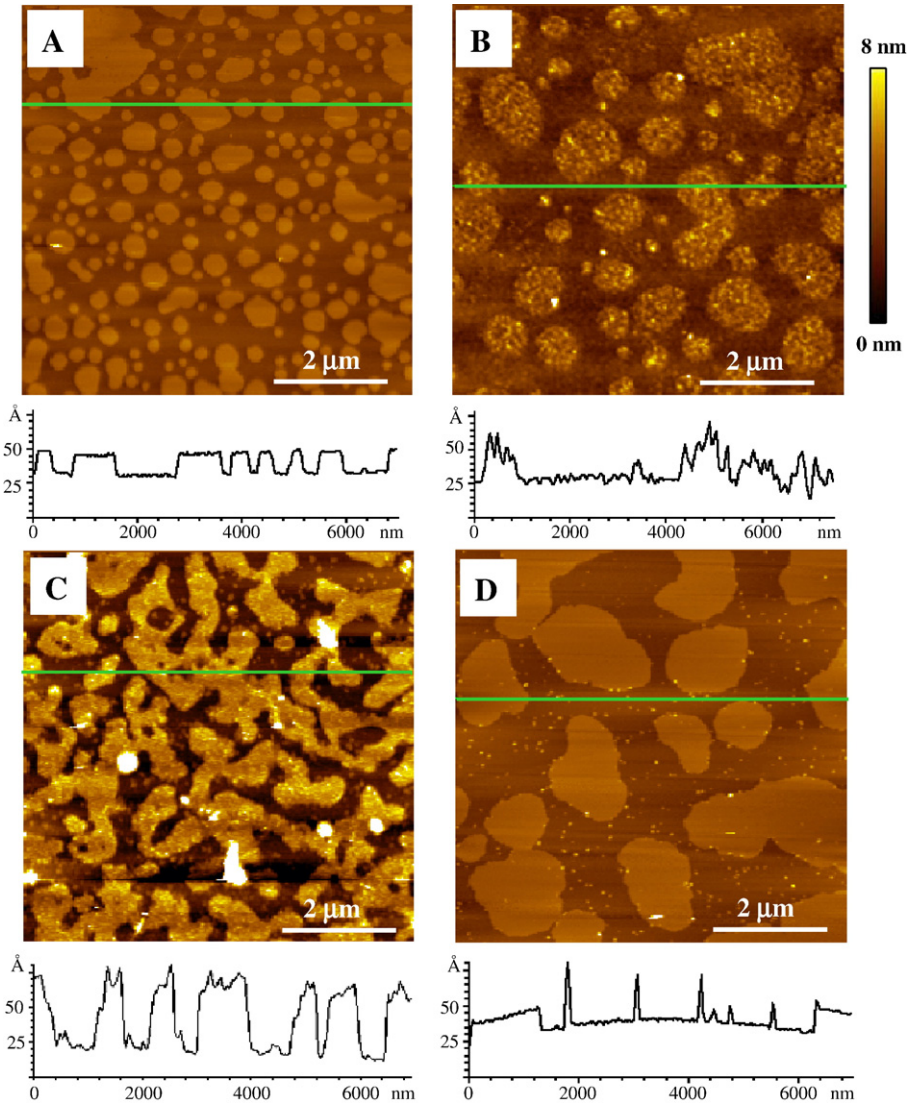

Fig. 2. Antibody binding identifies sulfoglycolipid domains. Atomic force microscopy images in aqueous solution for a 4:4:2:1 DPPC/PDPC/chol/SGG bilayer before (A) and after (B) incubation with anti-SGG/SGC and for 4:4:2:1 DPPC/PDPC/chol/SGC (C) and 4:4:2 DPPC/PDPC/chol (D) bilayers after incubation with anti-SGG/SGC. Cross-section analyses for the lines are shown beneath the individual images.

For comparison, we also prepared bilayers from a 4:4:2 DPPC/DOPC/chol mixture. Similar bilayer morphologies with raised domains of variable size and shape were obtained; however, the height between domains and the fluid phase was 1.0 nm (Fig. 1E), significantly less than that for PDPC mixtures, but in line with literature data for other ternary lipid raft mixtures [39–45]. There are several possible explanations for the larger height difference for the PDPC mixture. The highly unsaturated acyl chain for PDPC will significantly change the lipid conformation and packing and may lead to increased compressibility for the PDPC fluid phase. This will allow the AFM tip to penetrate further into the PDPC fluid phase (relative to DOPC), thus resulting in a larger apparent height difference between the domain and fluid phase. Changes in the relative partitioning of cholesterol between the two phases may also be different for the two mixtures. Addition of 9.1% SGG to DPPC/DOPC/chol bilayers gave smaller domains, very similar to observations for PDPC mixtures (Fig. 1F). These results provide an additional control to indicate that the results for sulfoglycolipid-containing mixtures are not influenced by contributions from possible lipid oxidation for PDPC-containing mixtures (see Experimental).

The surface areas covered by the domains for bilayers in the absence and presence of SGC and SGG are listed in Table 1. These are the results of the analyses of a number of images from three or more replicate sample preparations for each bilayer composition; the relatively large standard deviation reflects the variability in the domain size and shape observed for these samples. The area covered by the domains increases by 9 and 13% for SGC and SGG, respectively, consistent with localization of sulfoglycolipid in the liquid-ordered domains. The changes in domain morphology in the presence of the sulfoglycolipid are also in agreement with this hypothesis. SGG has saturated alkyl and acyl chains, both of which are predominantly C16:0. The acyl chains of SGC are a mixture of saturated (C24:0 for hydroxylated) and monounsaturated (C24:1 n-9 for non-hydroxylated). Thus, the primarily saturated chains of both SGG and SGC would be expected to interact preferentially with cholesterol and DPPC in the liquid-ordered domains. Based on the acyl chain lengths, SGC-rich domains would be expected to be higher than SGG-rich domains, in agreement with the above results. The reduction in domain height when SGG is added to the ternary lipid mixture may reflect interdigitation of the sulfoglycolipid, as observed previously in SGG liposomes [22], or a change in lipid packing or partitioning.

Table 1
Analysis of the surface area covered by domains in supported bilayers

Bilayer composition	Surface area covered by l_o domains (%)[a]	Surface area relative to control (%)
DPPC/PDPC/chol (2:2:1)—control	46±8	100
SGC/DPPC/PDPC/chol (0.5:4:4:2)	48±6	105
SGC/DPPC/PDPC/chol (1:4:4:2)	50±2	109
SGG/DPPC/PDPC/chol (1:4:4:2)	52±3	113
Sperm APM lipid extracts	20±3	44

[a] Data are expressed as mean ± S.D. calculated from ≥ 10 images (7 × 7 μm) of triplicate sample preparations for each bilayer.

We used affinity purified anti-SGC/SGG IgG, which binds specifically to both SGC and SGG, to confirm our hypothesis that the sulfoglycolipids are localized predominantly in the raft domains. Fig. 2A and B show images for the same DPPC/PDPC/chol/SGG bilayer before and after incubation with antibody. Upon incubation with anti-SGC/SGG IgG, there is a significant increase in both the surface roughness and the height of the l_o domains, which in some areas are 3–4 nm higher than the surrounding fluid phase. A small increase in heterogeneity of the fluid phase is also observed (see cross-section analysis in Fig. 2B) but it is much less pronounced than the change observed for the raft domains. Since different areas of the sample are imaged before and after the antibody incubation, there is some difference in domain size and shape in the images shown in Fig. 2A and B. However, this variability is typical for different areas of bilayers of the same sample.

A similar increase in domain heterogeneity and height is observed for DPPC/PDPC/chol/SGC bilayers after incubation with anti-SGC/SGG, as shown in Fig. 2C. These results indicate the localization of sulfoglycolipid in the l_o raft domains. The alteration of surface topography in the fluid phase may be due to either antibody binding to low concentrations of SGG/SGC in the fluid phase or non-specific binding of the antibody. Consistent with the latter possibility, incubation of a control DPPC/PDPC/chol bilayer (no SGC/SGG) with antibody showed some small raised features that are 3–4 nm in height in the fluid phase (Fig. 2D). Similarly, a small amount of non-specific binding was observed for a control in which a SGC-containing bilayer was incubated with PRS IgG (data not shown). In all cases the overall size and shape of the l_o domains for SGC/SGG containing bilayers are similar upon treatment with antibody, taking into account the fact that the same areas are not imaged before and after incubation with anti-SGC/SGG.

3.2. Localization of sulfoglycolipid in raft domains of APM lipid bilayers

AFM images of supported bilayers prepared from sperm APM lipid extracts revealed a number of small raised domains that range in size from 0.2–0.8 μm and are scattered randomly throughout the bilayer (Fig. 3A, D). The height of the domains is 1.6 ± 0.2 nm and both the domains and the surrounding bilayer matrix are more heterogeneous than the bilayers prepared from pure lipid mixtures (compare images in Figs. 1 and 3). There are only occasional small defects in the bilayer, clearly indicating an intact membrane with a mixture of coexisting phases, as opposed to bilayer patches or collapsed vesicles. The area covered by the domains (~20%, Fig. 3 and Table 1) is considerably lower than that obtained for the bilayers prepared from artificial lipid mixtures (Figs. 1 and 2) and primarily isolated, rather than interconnected, domains are observed.

Exposure of sperm APM lipid bilayers to anti-SGC/SGG IgG leads to an increase in the surface roughness and height of the domains, similar to the results obtained for model membranes (Fig. 3B, E). Topographical changes in the fluid

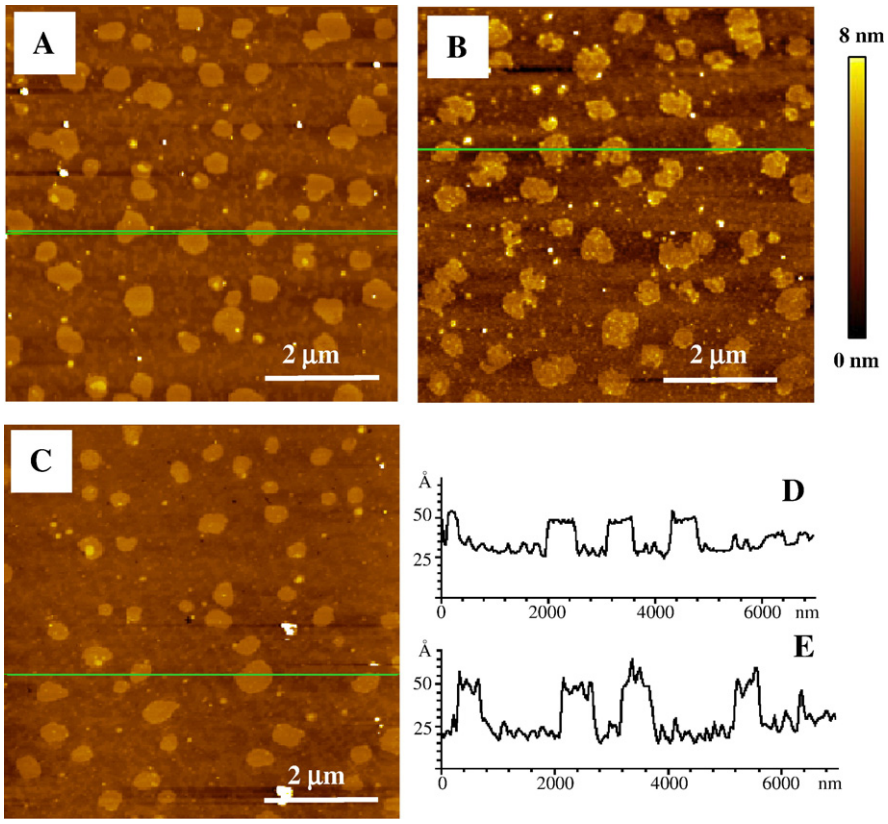

Fig. 3. Morphology of bilayers of lipid extracts from sperm anterior plasma membranes. Atomic force microscopy images of APM lipid extract bilayers in aqueous solution before (A) and after (B) incubation with anti-SGC/SGG and after incubation with PRS IgG (C). Cross-section analyses for images A and B are shown in D and E, respectively.

phase are not observed. A control experiment in which an APM lipid bilayer was exposed to PRS IgG (Fig. 3C) showed no change in domain morphology. This demonstrates the specificity of anti-SGC/SGG binding to the domains, thus indicating preferential localization of SGG in the lipid raft domains of sperm APM lipid bilayers.

3.3. Stability of bilayers treated with methyl-β-cyclodextrin

The cholesterol-sequestering agent, MβCD, has been widely used to modulate cholesterol content and disrupt lipid rafts in cellular studies [54,55]. It has also been shown to disrupt liquid-ordered domains in supported membranes prepared from synthetic lipid mixtures and cellular lipid extracts [43,45,56]. We first examined the effect of MβCD on the stability of DPPC/PDPC/chol bilayers. As shown in Fig. 4A, B, MβCD treatment results in a pronounced change in the domains, which have irregular boundaries and frequent areas of a lower phase in the center. The height difference between the domain and the surrounding bilayer matrix also increases by ~1 nm (Fig. 4C, D). Exposure of bilayers to MβCD for longer periods of time leads to increased heterogeneity and bilayer defects in both the domains and the fluid phase (data not shown).

Of particular interest, MβCD treatment of DPPC/PDPC/chol bilayers containing 9.1 mol% SGG also resulted in significant reorganization of the domains. As shown in Fig. 4E the periphery of the domains becomes less uniform after exposure to MβCD and the domains contain one or more small areas of lower phase (compare to untreated bilayer in Fig. 1D). The amount of lower phase within the domain is slightly lower than that observed for the ternary lipid mixtures in the presence of MβCD. The difference in height between the domain and fluid phase also increases (Fig. 4F) and the fluid phase becomes slightly more heterogeneous, possibly indicating the removal of lipid from the fluid phase. Similarly, for APM lipid extracts, treatment of bilayers with MβCD leads to pronounced changes in the bilayer morphology (Fig. 4G, H). In this case the domains are much smaller with irregular boundaries and significant heterogeneity in height and the surrounding fluid phase shows a higher surface roughness. Note that in many of the images in the presence of MβCD there are higher features (white dots in the images) due to excess lipid vesicles that are difficult to remove completely from the bilayers by washing prior to imaging.

3.4. Immunofluorescence detection of SGG microdomains in bilayers of APM lipids and APM vesicles

Supported bilayers prepared from APM vesicles had much higher surface roughness than bilayers prepared from either mixtures of pure lipids or extracted APM lipids. This presumably reflects both the presence of proteins in the APM membranes (which are removed during the extraction of the APM lipids) and problems in preparing uniform bilayers from the more heterogeneous natural membrane vesicles. The high

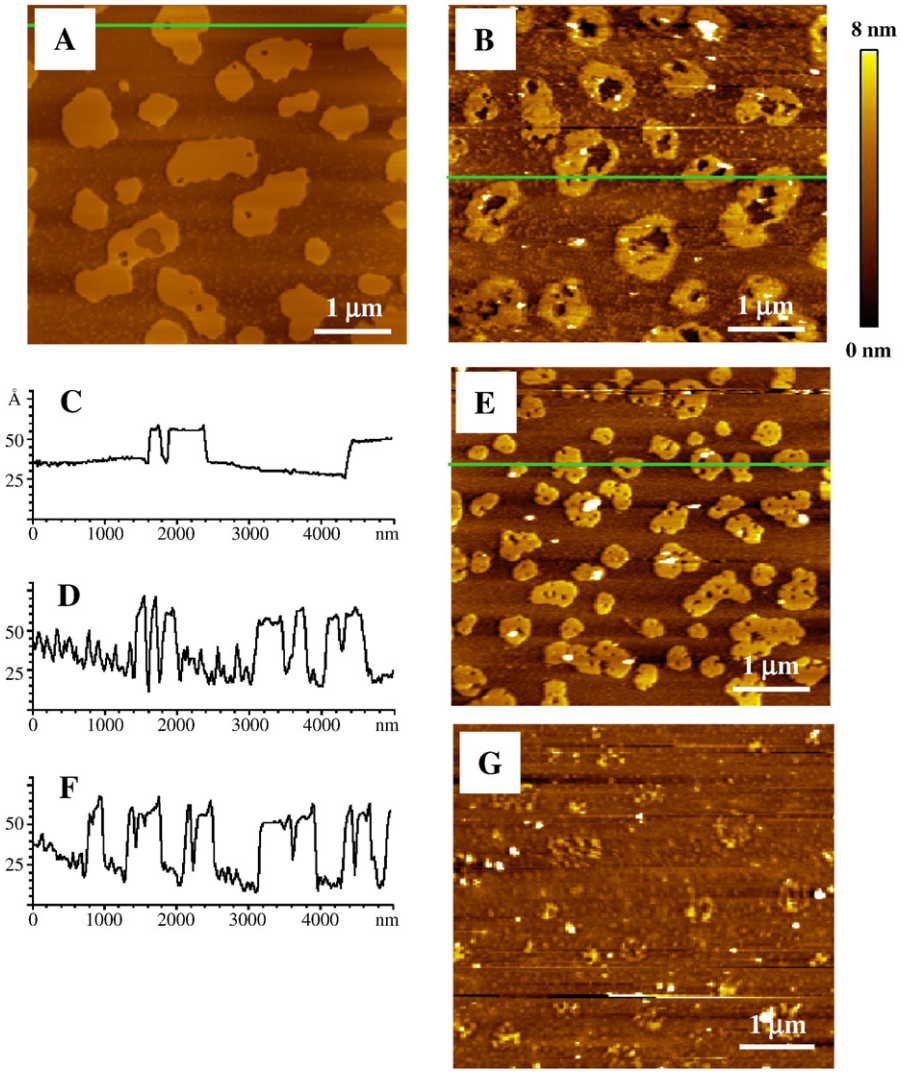

Fig. 4. Effects of MβCD on bilayers of artificial lipid mixtures and extracted APM lipids. Atomic force microscopy images and cross-section analyses for a 4:4:2 DPPC/PDPC/chol bilayer before (A, C) and after (B, D) incubation with MβCD. AFM images for 4:4:2:1 DPPC/PDPC/chol/SGG (E, cross-section in F) after incubation with MβCD. AFM images for APM lipid extract bilayers after (G) MβCD incubation. All incubations used 10 mM MβCD for 15 min.

surface roughness makes it difficult to use AFM measurements before and after incubation with anti-SGG to confirm the existence of the SGG-rich domains that are observed for purified APM lipids. Therefore, we used confocal microscopy to examine supported membranes prepared from lipids extracted from APM lipids and APM vesicles, after staining with anti-SGG IgG and Alexa-488-anti-rabbit IgG. The images obtained for APM lipids (Fig. 5A) show a large number of small bright islands, which vary in diameter from 0.3 to 0.7 µm (measured as the full width at half maximum of fluorescence intensity). This agrees with the domains observed for similar samples by AFM (Fig. 3, 0.2–0.8 µm; note the difference in scale between the confocal and AFM images); the latter technique, however, provides more accurate sizes for small domains that are below the diffraction-limited spatial resolution of confocal microscopy. Having demonstrated that the two methods give similar results for APM lipid extracts, we used immunofluorescence to probe for SGG-rich domains in supported membranes formed from APM vesicles. As shown in Fig. 5B, such membranes also show small fluorescent domains uniformly distributed throughout the membrane. Controls in which PRS is used in place of anti-SGG IgG reveal a higher level of background fluorescence for the APM vesicle membranes as compared to the APM lipids (data not shown).

4. Discussion

Our earlier studies have shown that SGG functions as a zona pellucida adhesion molecule and is found in sperm APMs that possess zona pellucida binding ability [28–30]. Furthermore, SGG has recently been isolated as part of the detergent-resistant membrane fraction from sperm and has been shown to cluster in the sperm head plasma membrane [28]. The possible role for SGG-rich lipid rafts in modulating sperm–egg interactions warrants an investigation of the localization of SGG in raft model membranes and sperm APMs. In the present work we provide definitive evidence for the localization of SGG and its structural analog SGC in liquid-ordered raft domains in model

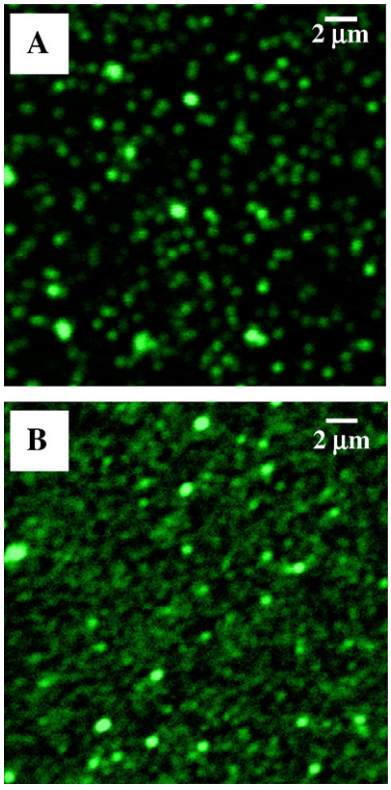

Fig. 5. Immunofluorescence confirms the presence of SGG domains. Confocal fluorescence images of bilayers prepared from APM lipid extracts (A) and APM vesicles (B). Bilayers were incubated with anti-SGC/SGG and Alexa-488 nm conjugated secondary antibody prior to imaging.

membranes. More importantly, we demonstrate that SGG-rich microdomains are observed by both AFM and immunofluorescence microscopy in membranes of sperm APM vesicles and their extracted lipids. In this work we have taken advantage of the capabilities of AFM for examining membrane morphology on the submicron length scale in aqueous solution.

The ternary lipid mixture that we have used to model the sperm anterior head plasma membrane was selected on the basis of the isolation of SGG and DPPC as the main saturated lipids in detergent-resistant membranes [28] and the observation that PDPC is the most prevalent polyunsaturated phospholipid in mammalian sperm [24,51]. AFM shows that supported bilayers of DPPC/PDPC/chol exhibit phase separation to give liquid-ordered domains that are enriched in DPPC and chol and are surrounded by a fluid PDPC-rich phase. These results are very similar to those that have been obtained in AFM studies of other ternary lipid mixtures, such as SM or DPPC with chol and a fluid PC [39,41,42]. Lateral phase separation has also been observed for mixtures of SM, chol and palmitoyldocosahexaenoylphosphoethanolamine [57]. The size, shape and degree of interconnectivity of the domains are quite variable, both for different areas of the same sample and for different samples, in many of these studies [41,42,45,53]. This may reflect small changes in the lipid ratios and in the conditions for vesicle fusion to form a supported membrane. The structural diversity of sphingomyelin domains and the effects of additives such as dye-labeled phospholipids on condensed domains have been recently studied in some detail [58,59]. Furthermore, the thermal history of the sample can have pronounced effects on bilayer domain morphology [60].

The addition of up to 9% SGC and SGG to the ternary lipid mixtures leads to changes in the size and interconnectivity of domains and increases their fractional coverage of the bilayer surface. Interestingly the largest effects are observed upon addition of 9% SGG (similar to the physiological concentration found in sperm lipid extracts [28]) which leads to distinctly smaller and less interconnected domains. Previous studies have shown that domain sizes in model membranes are controlled by a combination of line tension and dipole effects [52]; it is likely that electrostatic effects and hydrogen bonding are the main factors determining the size of sulfoglycolipid-containing domains. The changes in membrane morphology are not sufficient to demonstrate unequivocally that the sulfoglycolipid is localized in the liquid-ordered phase, in the absence of a more quantitative approach for analyzing the variable domains that we observe. However, the antibody labeling experiments clearly demonstrate that most of the sulfoglycolipid is in the domains, even at the relatively high concentration of 9%. This is also consistent with the strong hydrogen bonding interactions between SGG (or SGC) and cholesterol [28]. Incubation with anti-SGC/SGG leads to a heterogeneous distribution of small aggregates of antibody that cover a significant fraction (but not all) of the domains. This incomplete labeling may reflect a non-uniform distribution of SGG within the liquid-ordered domains, consistent with the fact that there is a wider distribution of domain heights in the presence of sulfoglycolipid than for the ternary lipid mixture alone. Small clusters and filaments of other glycolipids such as GM1 within liquid-ordered or gel phase domains have been observed by AFM for both supported monolayers and bilayers [16–18,61].

Incubation with MβCD leads to significant changes in the DPPC/PDPC/chol bilayers alone and in the presence of SGG. Both the domains and the fluid phase become more heterogeneous and the height difference between the two phases increases. The reorganization of the domains is more pronounced (for the same MβCD concentration and exposure time) for bilayers in the absence of SGG. This suggests that sulfoglycolipid imparts additional stability to the liquid-ordered domains, consistent with the strong interactions between SGG and chol [28] leading to tighter lipid packing within the domains. There are several possible explanations for the increased heights of the domains in the presence of MβCD, including (1) the retention of MβCD on the domains, (2) restructuring of the lipids remaining after chol removal to give a thicker gel phase membrane domain and (3) removal of chol from the fluid phase, thereby reducing its packing and height. The fact that both domains and fluid phase change upon MBCD treatment suggests that cholesterol is removed from both. This is in line with several recent AFM studies which have used MβCD or a chol-MβCD complex for the *in situ* manipulation of chol content in bilayers of binary and ternary lipid mixtures [42,43,56]. These results demonstrate that a variety of changes occur in membrane morphology as a function of [MβCD] and time, including the formation of membrane defects, and have

been rationalized by cyclodextrin-mediated exchange of chol and other phospholipids between gel, liquid-ordered and fluid phases. In some cases MβCD has been shown to extract lipids other than chol (e.g., SM) from bilayers [56,62], further complicating the analysis of its effects on membrane domains. Despite the complex changes induced by MβCD, there is good agreement between the results for supported membranes and our previous work. The latter showed that treatment of sperm with 5 mM MβCD did not change the amount of the lipid raft fraction isolated whereas 10 mM MβCD gave a 30% decrease in the yield of isolated lipid rafts with 50% of the sperm dead after MβCD treatment (N. Tanphaichitr, unpublished results).

Supported bilayers of lipids extracted from the sperm anterior head plasma membrane have a strikingly similar morphology to those obtained from the artificial lipid mixtures. The microdomains are slightly smaller in size but similar in height to those obtained for 9% SGG in a DPPC/PDPC/chol bilayer. It is particularly noteworthy that the addition of SGG actually leads to smaller more distinct microdomains than are observed from the ternary mixtures alone and results in a bilayer morphology that closely resembles that obtained for the APM lipid membranes. The antibody labeling experiments clearly demonstrate that the majority, if not all, of the SGG is localized in the domains. This observation and the pronounced effect of the chol sequestering agent MβCD strongly support the assignment of these microdomains to liquid-ordered, sulfoglycolipid-rich membrane rafts. The fluid phase in the APM lipid membranes is significantly more heterogeneous than that in the bilayers prepared from artificial lipid mixtures. This is reasonable based on the expected heterogeneity in lipid chain length in the APM extracts. The microdomains cover ~22% of the surface for the APM lipid bilayers, approximately half that obtained in the ternary lipid mixtures containing SGG. This suggests that the APM lipid extracts have a significantly different ratio of saturated to unsaturated phospholipids from the 1:1 DPPC/PDPC ratio used for the model membranes. This is supported by literature results showing that sperm membrane phospholipids are comprised of 70% unsaturated and 20% saturated fatty acid acyl chains [51].

The results obtained in the present work for the APM lipid extracts can be compared to an earlier study of phase separation in extracted lipid mixtures. In this case, hybrid supported bilayers with extracted brush border membrane lipids in the top leaflet were shown by fluorescence microscopy to form relatively large (~1–5 μm in diameter) liquid-ordered domains that were similar to those observed using ternary mixtures of synthetic lipids [45,63]. Our results are similar, except that the domains are much smaller than those observed by fluorescence for the brush border membranes. The small domains are considerably closer to what is expected for rafts in cells, suggesting that supported bilayers can mimic some of the characteristics of rafts in natural membranes. For supported bilayers prepared from mixtures of pure lipids the domains are coupled through both bilayer leaflets, by contrast to the hybrid supported bilayers examined in the earlier study [45]. The bilayers prepared from APM lipids have more heterogeneous domains which may indicate that the detergent-free extraction method used to isolate APM vesicles maintains some of the natural asymmetry of the sperm plasma membrane.

The immunofluorescence experiments demonstrate that similar sulfoglycolipid-rich domains are present in supported bilayers prepared from sperm APM lipids and APM vesicles. The sizes of these domains (0.3 to 0.7 μm) are similar to those of sperm APM lipid bilayers as determined by AFM (0.2 to 0.7 μm). These results, as well as those for the SGG-containing model membranes, are consistent with the hypothesis that SGG is localized *in situ* in lipid raft domains in sperm APMs. They also agree with previous observations of SGG clusters on the sperm head plasma membrane of live gametes, as shown by indirect immunofluorescence [28,29].

It is likely that the second T_m of isolated ram sperm APMs (~60 °C), in addition to the lower T_m of 26 °C, can be assigned to the lipid raft domains [64], which contain ordered lipids, SGG and saturated phospholipids [28]. Isolated sperm lipid rafts contain SGG and ZP binding proteins [28,65–67] and thus have direct affinity for the ZP [28]. Sperm continue to swim during the interaction between the sperm head anterior and the ZP. Therefore, it is possible that the liquid-ordered property of the raft domains, which contain a number of ZP binding molecules, in the sperm head anterior is beneficial for this gamete interaction, since it provides stability against the pulling force of the moving sperm [68]. The ZP binding molecules located in sperm lipid rafts may act cooperatively, thus enhancing their affinity to the ZP. The presence of multiple SGG molecules in sperm head plasma membrane lipid rafts will also enhance the interaction of the sulfoglycolipid with the ZP glycan via a "Velcro" mechanism. Due to the multivalent glycan moieties of each ZP glycoprotein, the interaction of these ZP glycans with SGG and other ZP binding molecules in sperm lipid rafts may lead to aggregation of lipid rafts to form macrorafts that initiate cell signaling events [69].

Acknowledgements

WW acknowledges support from the National Research Council Canada–Thailand Research Fund Exchange Program for a postdoctoral fellowship. NT acknowledges CIHR and NSERC for support. KK receives a scholarship from the Development and Promotion of Science and Technology Talented Project Thailand.

References

[1] K. Simons, E. Ikonen, Functional rafts in cell membranes, Nature 387 (1997) 569–572.
[2] K. Simons, E. Ikonen, How cells handle cholesterol, Science 290 (2000) 1721–1726.
[3] D.A. Brown, E. London, Structure and function of sphingolipid- and cholesterol-rich membrane rafts, J. Biol. Chem. 275 (2000) 17221–17224.
[4] D.A. Brown, E. London, Functions of lipid rafts in biological membranes, Annu. Rev. Cell Dev. Biol. 14 (1998) 111–136.
[5] R.G.W. Anderson, K. Jacobson, A role for lipid shells in targeting proteins to caveolae, rafts and other lipid domains, Science 296 (2002) 1821–1825.
[6] A. Kusumi, C. Nakada, K. Ritchie, K. Murase, K. Suzuki, H. Murakoshi, R.S. Kasai, J. Kondo, T. Fujiwara, Paradigm shift of the plasma membrane concept from the two-dimensional continuum fluid to the partitioned fluid:

high speed single molecule tracking of membrane molecules, Annu. Rev. Biophys. Biomol. Struct. 34 (2005) 351–378.
[7] A. Laude, I.A. Prior, Plasma membrane microdomains: organization, function and trafficking, Mol. Memb. Biol. 21 (2004) 193–205.
[8] F.R. Maxfield, Plasma membrane microdomains, Curr. Opin. Cell Biol. 14 (2002) 483–487.
[9] S. Munro, Lipid rafts: elusive or illusive, Cell 115 (2003) 377–388.
[10] L.J. Pike, Lipid rafts: heterogeneity on the high seas, Biochem. J. 378 (2004) 281–292.
[11] K. Simons, W.L. Vaz, Model systems, lipid rafts and cell membranes, Annu. Rev. Biophys. Biomol. Struct. 33 (2004) 269–295.
[12] M. Edidin, The state of lipid rafts: from model membranes to cells, Annu. Rev. Biophys. Biomol. Struct. 32 (2003) 257–283.
[13] P. Burgos, C. Yuan, M.-L. Viriot, L.J. Johnston, Two-color near-field fluorescence microscopy studies of microdomains ("rafts") in model membranes, Langmuir 19 (2003) 8002–8009.
[14] J. Murray, L. Cuccia, A. Ianoul, J.C. Cheetham, L.J. Johnston, Imaging the selective binding of synapsin to anionic membrane domains, ChemBioChem 5 (2004) 1–6.
[15] A. Ianoul, P. Burgos, Z. Lu, R.S. Taylor, L.J. Johnston, Phase separation and interlayer coupling in complex supported phospholipid bilayers visualized by near-field scanning optical microscopy in liquid, Langmuir 19 (2003) 9246–9254.
[16] C. Yuan, J. Furlong, P. Burgos, L.J. Johnston, The size of lipid rafts: an atomic force microscopy study of ganglioside GM1 domains in sphingomyelin/DOPC/cholesterol membranes, Biophys. J. 82 (2002) 2526–2535.
[17] C. Yuan, L.J. Johnston, Distribution of ganglioside GM1 in L-α-dipalmitoylphosphatidylcholine/cholesterol monolayers: a model for lipid rafts, Biophys. J. 79 (2000) 2768–2781.
[18] C. Yuan, L.J. Johnston, Atomic force microscopy studies of ganglioside GM1 domains in phosphatidylcholine and phosphatidylcholine/cholesterol bilayers, Biophys. J. 81 (2001) 1059–1069.
[19] A. Ianoul, M. Street, D. Grant, J. Pezacki, R. Taylor, L.J. Johnston, Near field scanning fluorescence microscopy study of ion channel clusters in cardiac myocyte membranes, Biophys. J. 87 (2004) 3525–3535.
[20] A. Ianoul, D.D. Grant, Y. Rouleau, M. Bani-Yaghoub, L.J. Johnston, J.P. Pezacki, Imaging nanometer domains of β-adrenergic receptor complexes on the surface of cardiac myocytes, Nat. Chem. Biol. 1 (2005) 196–202.
[21] S.G. Boxer, Molecular transport and organization in supported lipid membranes, Curr. Opin. Chem. Biol. 4 (2000) 704–709.
[22] M. Attar, M. Kates, M. Bou Khalil, D. Carrier, P.T.T. Wong, N. Tanphaichitr, A Fourier transform infrared study of the interaction between germ-cell specific sulfogalactosylglycerolipid and dimyristoylglycerophosphocholine, Chem. Phys. Lipids 106 (2000) 101–114.
[23] M. Attar, P.T. Wong, M. Kates, D. Carrier, P. Jaklis, N. Tanphaichitr, Interaction between sulfogalactosylceramide and dimyristoylphosphatidylcholine increases the orientational fluctuation of their lipid hydrocarbon chains, Chem. Phys. Lipids 94 (1998) 227–238.
[24] N. Tanphaichitr, M. Bou Khalil, W. Weerachatyankul, M. Kates, H. Xu, E. Carmona, M. Attar, D. Carrier, in: S. De Vries (Ed.), Lipid metabolism and male fertility, AOCS Press, Champaign, IL, 2003, pp. 125–148.
[25] D.A. Brown, J.K. Rose, Sorting of GPI-anchored proteins to glycolipid-enriched membrane subdomains during transport to apical cell surface, Cell 68 (1992) 533–544.
[26] K. Ohta, C. Sato, T. Matsuda, M. Toriyama, W. Lennarz, K. Kitajima, Isolation and characterization of low density detergent-insoluble membrane (LD-DIM) fraction from sea urchin sperm, Biochem. Biophys. Res. Commun. 258 (1999) 616–623.
[27] I. Ishizuka, Chemistry and functional distribution of sulfoglycolipids, Prog. Lipid Res. 36 (1997) 245–319.
[28] M. Bou Khalil, K. Chakrabandhu, M. Buhr, T. Berger, H. Xu, N. Vuong, P. Kumarathasan, E. Carmona, P.T.T. Wong, D. Carrier, N. Tanphaichitr, Sperm capacitation induces an increase in lipid rafts having zona pellucida binding ability and containing sulfogalactosylglycerolipid, Dev. Biol. 290 (2006) 220–235.
[29] D. White, W. Weerachatyanukul, B. Gadella, N. Kamolvarin, M. Attar, N. Tanphaichitr, Role of sperm sulfogalactosylglycerolipid in mouse sperm-zona pellucida binding, Biol. Reprod. 63 (2000) 147–155.
[30] W. Weerachatyanukul, M. Rattanachaiyanont, E. Carmona, A. Furimsky, A. Mai, A. Shoushtarian, S. Sirichotiyakul, H. Ballakier, A. Leader, N. Tanphaichitr, Sulfogalactosylglycerolipid is involved in human gamete interaction, Mol. Reprod. Dev. 60 (2001) 569–578.
[31] S. Tupper, P.T.T. Wong, N. Tanphaichitr, Binding of Ca^{2+} to sulfogalactosylceramide and the sequential effects on the lipid dynamics, Biochemistry 31 (1992) 11902–11907.
[32] M. Kates, in: R.H. Burdon (Ed.), Laboratory techniques in Biochemistry and Molecular Biology, Elsevier, New York, 1986, pp. 100–278.
[33] S. Tupper, P.T.T. Wong, M. Kates, N. Tanphaichitr, Interaction of divalent cations with germ cell specific sulfogalactosylglycerolipid and the effects on lipid chain dynamics, Biochemistry 33 (1994) 13250–13258.
[34] C.S. Melendrez, S. Meizel, T. Berger, Comparison of the ability of progesterone and heat solubilized porcine zona pellucida to initiate the porcine sperm acrosome reaction in vitro, Mol. Reprod. Dev. 39 (1994) 433–438.
[35] R.A. Harrison, B. Mairet, N.G. Miller, Flow cytometric studies of bicarbonate-mediated Ca^{2+} influx in boar sperm population, Mol. Reprod. Dev. 35 (1993) 197–208.
[36] R. Peterson, L. Russell, D. Bundman, M. Freund, Evaluation of the purity of boar sperm plasma membranes prepared by nitrogen cavitation, Biol. Reprod. 23 (1980) 637–645.
[37] E.G. Bligh, W.J. Dyer, A rapid method of total lipid extraction and purification, Can. J. Med. Sci. 37 (1959) 911–917.
[38] A. Furimsky, N. Vuong, H. Xu, P. Kumarathasan, M. Xu, W. Weerachatyanukul, M. Bou Khalil, M. Kates, N. Tanphaichitr, Percoll-gradient centrifuged capacitated mouse sperm have increased fertilizing ability and higher contents of sulfogalactosylglycerolipid and docasahexaenoic acid-containing phosphatidylcholine than washed capacitated mouse sperm, Biol. Reprod. 72 (2005) 574–583.
[39] F. Tokumasu, A.J. Jin, G.W. Feigenson, J.A. Dvorak, Nanoscopic lipid domain dynamics revealed by atomic force microscopy, Biophys. J. 84 (2003) 2609–2618.
[40] B.Y. van Duyl, D. Ganchev, V. Chupin, B. de Kruijff, J.A. Killian, Sphingomyelin is much more effective than saturated phosphatidylcholine in excluding unsaturated phosphatidylcholine from domains formed with cholesterol, FEBS Lett. 547 (2003) 101–106.
[41] D.E. Saslowsky, J. Lawrence, X. Ren, D.A. Brown, R.M. Henderson, J.M. Edwardson, Placental alkaline phosphatase is efficiently targeted to rafts in supported lipid bilayers, J. Biol. Chem. 277 (2002) 26966–26970.
[42] P.-E. Milhiet, M.-C. Giocondi, O. Baghdadi, F. Ronzon, B. Roux, C. Le Grimellec, Spontaneous insertion and partitioning of alkaline phosphatase into model lipid rafts, EMBO Rep. 3 (2002) 485–490.
[43] J.C. Lawrence, D.E. Saslowsky, J.M. Edwardson, R.M. Henderson, Real time analysis of the effects of cholesterol on lipid raft behavior using atomic force microscopy, Biophys. J. 84 (2003) 1827–1832.
[44] J.M. Crane, L.K. Tamm, Role of cholesterol in the formation and nature of lipid rafts in planar and spherical model membranes, Biophys. J. 86 (2004) 2965–2979.
[45] C. Dietrich, L.A. Bagatolli, Z.N. Volovyk, N.L. Thompson, M. Levi, K. Jacobson, E. Gratton, Lipid rafts reconstituted in model membranes, Biophys. J. 80 (2001) 1417–1428.
[46] K. Bacia, P. Schwille, T. Kurzchalla, Sterol structure determines the separation of phases and the curvature of the liquid-ordered phase in model membranes, Proc. Natl. Acad. Sci. 102 (2005) 3272–3277.
[47] A.T. Hammond, F.A. Heberle, T. Baumgart, D. Holowka, B. Baird, G.W. Feigenson, Crosslinking a lipid raft component triggers liquid ordered-liquid disordered phase separation in model plasma membranes, Proc. Natl. Acad. Sci. 101 (2005) 6320–6325.
[48] A.V. Samsonov, I. Mihalyov, F.S. Cohen, Characterization of cholesterol-sphingomyelin domains and their dynamics in bilayer membranes, Biophys. J. 81 (2001) 1486–1500.
[49] B.L. Stottrup, S.L. Veatch, S.L. Keller, Nonequilibrium behavior in supported lipid membranes containing cholesterol, Biophys. J. 86 (2004) 2942–2950.
[50] S.L. Veatch, S.L. Keller, Separation of liquid phases in giant vesicles of ternary mixtures of phospholipids and cholesterol, Biophys. J. 85 (2003) 3074–3083.

[51] J.E. Parks, D.V. Lynch, Lipid composition and thermotropic phase behavior of boar, bull, stallion and rooster sperm membranes, Cryobiology 29 (1992) 255–256.
[52] V.T. Moy, D.J. Keller, H.E. Gaub, H.M. McConnell, Long-range molecular orientational order in monolayer solid domains of phospholipids, J. Phys. Chem. 90 (1986) 3198–3202.
[53] H.A. Rinia, M.M.E. Snel, J.P.J.M. van der Eerden, B. de Kruijff, Visualizing detergent resistant domains in model membranes with atomic force microscopy, FEBS Lett. 501 (2001) 92–96.
[54] M. Hao, S. Mukherjee, F.R. Maxfield, Cholesterol depletion induces large scale domain segregation in living cell membranes, Proc. Natl. Acad. Sci. 98 (2001) 13072–13077.
[55] P. Scheiffele, M.G. Roth, K. Simons, Interaction of influenza virus haemagglutinin with sphingolipid microdomains of the plasma membrane, EMBO J. 16 (1997) 5501–5508.
[56] M.-C. Giocondi, P.E. Milhiet, P. Dosset, C. Le Grimellec, Use of cyclodextrin for AFM monitoring of model raft formation, Biophys. J. 86 (2004) 861–869.
[57] S.R. Shaikh, A.C. Dumaual, A. Castillo, D. LoCascio, R.A. Siddiqui, W. Stillwell, S.R. Wassall, Oleic and docosahexaenoic acid differentially phase separate from lipid raft molecules: a comparative NMR, DSC, AFM and detergent extraction study, Biophys. J. 87 (2004) 1752–1766.
[58] A. Cruz, L. Vazquez, M. Velez, J. Perez-Gil, Influence of a fluorescent probe on the nanostructure of phospholipid membranes: dipalmitoylphosphatidylcholine interfacial monolayers, Langmuir 21 (2005) 5349–5355.
[59] M.-C. Giocondi, S. Boichot, T. Plenat, C. Le Grimellec, Structural diversity of sphingomyelin microdomains, Ultramicroscopy 100 (2004) 135–143.
[60] W.-C. Lin, C.D. Blanchette, T.V. Ratto, M.L. Longo, Lipid asymmetry in DLPC/DSPC-supported lipid bilayers: a combined AFM and fluorescence microscopy study, Biophys. J. 90 (2006) 228–237.
[61] V. Vie, N.V. Mau, E. Lesniewska, J.P. Goudonnet, F. Heitz, C. Le Grimellec, Distribution of ganglioside GM1 between two-component, two-phase phosphatidylcholine monolayers, Langmuir 14 (1998) 4574–4583.
[62] S.-L. Niu, D.C. Mitchell, B.J. Litman, Manipulation of cholesterol levels in rod disk membranes by methyl-β-cyclodextrin, J. Biol. Chem. 277 (2002) 20139–20145.
[63] C. Dietrich, Z.N. Volovyk, M. Levi, N.L. Thompson, K. Jacobson, Partitioning of Thy-1, GM1 and cross-linked phospholipid analogs into lipid rafts reconstituted in supported model membrane monolayers, Proc. Natl. Acad. Sci. 98 (2001) 10642–10647.
[64] D.E. Wolf, V.M. Maynard, C.A. McKinnon, D.L. Melchior, Lipid domains in the ram sperm plasma membrane demonstrated by differential scanning calorimetry, Proc. Natl. Acad. Sci. 87 (1990) 6893–6896.
[65] H. Nishimura, C. Cho, D.R. Branciforte, D.G. Myles, P. Primakoff, Analysis of loss of adhesive function in sperm lacking cyritestin or fertilin beta, Dev. Biol. 233 (2001) 204–213.
[66] S.B. Sleight, P.V. Miranda, N.-W. Plaskett, B. Maier, J. Lysiak, H. Scrable, J.C. Herr, P.E. Visconti, Isolation and proteomic analysis of mouse sperm detergent-resistant membrane fractions. Evidence for dissociation of lipid rafts during capacitation, Biol. Reprod. 73 (2005) 721–729.
[67] R.A. van Gestel, I.A. Brewis, P.R. Ashton, J.B. Helms, J.F. Brouwers, B. M. Gadella, Capacitation-independent concentration of lipid rafts in the apical ridge head area of porcine sperm cells, Mol. Human Reprod. 11 (2005) 583–590.
[68] J.M. Baltz, D.F. Katz, R.A. Cone, Mechanics of sperm–egg interaction at the zona pellucida, Biophys. J. 54 (1988) 643–654.
[69] K. Simons, R. Ehehalt, Cholesterol, lipid rafts and disease, J. Clin. Invest. 110 (2002) 597–603.